Nanoscale Magnetic Structure of Ferromagnet/Antiferromagnet Manganite Multilayers

D. Niebieskikwiat,[1,2] L. E. Hueso,[3,4] J. A. Borchers,[5] N. D. Mathur,[3] and M. B. Salamon[1,*]

[1]*Department of Physics, University of Illinois at Urbana-Champaign, Urbana, Illinois 61801, USA*
[2]*Colegio de Ciencias e Ingeniería, Universidad San Francisco de Quito, Quito, Ecuador*
[3]*Department of Materials Science, University of Cambridge, Cambridge CB2 3QZ, United Kingdom*
[4]*Department of Physics and Astronomy, University of Leeds, Leeds LS2 9JT, United Kingdom*
[5]*NIST Center for Neutron Research, National Institute of Standards and Technology, Gaithersburg, Maryland 20899, USA*

(Received 13 February 2007; published 14 December 2007)

We use polarized neutron reflectometry and dc magnetometry to obtain a comprehensive picture of the magnetic structure of a series of $La_{2/3}Sr_{1/3}MnO_3/Pr_{2/3}Ca_{1/3}MnO_3$ (LSMO/PCMO) superlattices, with varying thickness of the antiferromagnetic (AFM) PCMO layers ($0 \leq t_A \leq 7.6$ nm). While LSMO presents a few magnetically frustrated monolayers at the interfaces with PCMO, in the latter a magnetic contribution due to ferromagnetic (FM) inclusions within the AFM matrix is maximized at $t_A \sim 3$ nm. This enhancement of FM moment occurs at the matching between layer thickness and cluster size, implying the possibility of tuning phase separation by imposing appropriate geometrical constraints which favor the accommodation of FM nanoclusters within the ''non-FM'' material.

DOI: 10.1103/PhysRevLett.99.247207 PACS numbers: 75.70.Cn, 61.12.Ha, 75.70.Kw

Nanostructured magnetic materials are already finding applications in magnetic recording and memory devices. One important focus has been on tunneling magnetoresistance (TMR), in which ferromagnetic (FM) layers having spin-polarized conduction electrons are separated by a nonmagnetic insulating barrier [1]. TMR occurs when the applied field aligns the magnetic moments of the FM layers, allowing the spin-polarized tunneling of carriers through the insulator. Spin-polarized double-exchange magnets such as $La_{2/3}(Sr, Ca)_{1/3}MnO_3$ have been considered as the metallic layers, along with various insulating barriers such as $SrTiO_3$ (STO), $LaAlO_3$, $NdGaO_3$. The results are not encouraging, probably because the interfacial magnetization falls off with increasing temperature more rapidly than does the bulk magnetization [1].

As a different approach to TMR devices, we have fabricated all-manganite multilayers utilizing antiferromagnetic (AFM) insulating manganites as the barrier [2–5]. In these multilayers, we first expect that the similarities in lattice structure and stoichiometry at the manganite-manganite interfaces will minimize the suppression of interfacial magnetization. We next explore the possibility of inducing magnetization in the AFM spacer and thereby having a magnetic-field-sensitive tunnel barrier, which would contribute to the TMR effect. AFM materials with FM instabilities (phase-separated manganites) are thus ideal candidates for the insulating layers [6].

We use as the barrier layer $Pr_{2/3}Ca_{1/3}MnO_3$ (PCMO), which supports nanoscale FM droplets within its AFM insulating matrix [7–9]. Because of its high Curie temperature, we use $La_{2/3}Sr_{1/3}MnO_3$ (LSMO) for the FM layers. We report the magnetic properties as functions of temperature and spacer-layer thickness, using polarized neutron reflectivity (PNR) to map the magnetization profile through the multilayer structure. Despite the structural regularity of the interfaces, magnetically disordered regions appear at the surfaces of the LSMO layers. In contrast, the FM moment is enhanced in the PCMO spacer when its layer thickness is ~3 nm. Interestingly, this is the situation where the layer thickness matches the size of the FM clusters that occur in PCMO [9].

Epitaxial superlattices were grown on atomically flat STO (001) substrates by pulsed laser deposition at 750 °C. Then, the films were annealed at 750 °C in 60 kPa of oxygen for 1 h. The multilayers involve five repetitions of LSMO/PCMO bilayers, with LSMO as the starting layer. The thicknesses obtained from x-ray diffraction and PNR (accuracy 0.1 nm) are 11.9 nm for LSMO (in all cases), while for PCMO they are $t_A = 0$, 0.8, 1.7, 2.7, 3.5, 4.3, and 7.6 nm, respectively (for $t_A = 0$, a single 11.9-nm-thick layer of LSMO was grown). The out-of-plane lattice parameters (3.85 and 3.76 Å for LSMO and PCMO, respectively) are smaller than the bulk values (3.88 and 3.83 Å, respectively), confirming the tensile stress imposed by the substrate (the in-plane lattice parameter is 3.90 Å for all STO, LSMO, and PCMO).

Magnetization (M) data were obtained in a SQUID magnetometer, with in-plane magnetic fields $\mu_0 H \leq 7$ T. $M(H)$ loops at $T = 5$ K for three selected samples are shown in Fig. 1. All our multilayers show sharp FM loops, with a Curie temperature $T_C \sim 345$ K (obtained from M vs T) corresponding to the LSMO layers. A close inspection of these data reveals a small but clear variation of the magnetic moment with the thickness t_A. After correcting for a minor substrate contribution [10], we obtained the spontaneous magnetization M_0 (the back extrapolation to $H = 0$ from the high-field saturated region). Since only FM phases can give a spontaneous moment, M_0 is a direct measure of the FM volume of the samples [11]. Two curious features can be noticed in M_0 vs t_A [Fig. 2(a)].

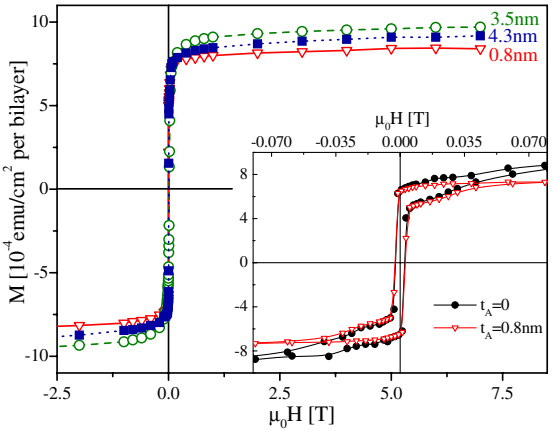

FIG. 1 (color online). Magnetization loops at $T = 5$ K for three selected samples (1 emu $= 10^{-3}$ A m^2). The labels indicate the thickness of the $Pr_{2/3}Ca_{1/3}MnO_3$ layers (t_A). Inset: Low-field region of the same loops for $t_A = 0$ and 0.8 nm.

At $t_A = 0$, M_0 corresponds to the saturation of pure LSMO, but then the moment decreases when a thin layer of PCMO ($t_A = 0.8$ nm) is added between the LSMO layers. The decrease of M_0 suggests a reduction of the magnetic moment of the LSMO, since any FM contribution from the PCMO should align parallel to the applied field (this is indeed confirmed by PNR). For thicker PCMO layers M_0 increases again due to the contribution of FM droplets inside the PCMO [2,6–9].

Clearly, an AFM coupling between different LSMO layers cannot be responsible for the initial reduction of M_0. RKKY-like interactions require a nonmagnetic metallic intermediate layer [12], which is not the case for PCMO, and weak dipolar interactions could hardly induce this behavior. In both cases the applied field should realign the magnetic moments of the LSMO layers. However, M_0 stays the same even after cooling the samples under a high field of 7 T. Differently, a plausible reason for the reduction of M_0 is the formation of magnetically disordered regions at the LSMO side of the FM-AFM interfaces, as it has been observed in other systems [1,13,14].

While $M(H)$ measurements are not conclusive about the origin of the reduction of M_0, PNR provides a depth profile of M and is thus an ideal tool to test for the existence of disordered interfaces [13,14]. PNR experiments were carried out on the NG1 reflectometer at the NIST Center for Neutron Research at $T = 6$, 120, and 300 K on three selected samples, $t_A = 1.7$, 2.7, and 4.3 nm. An in-plane magnetic field of 0.32 T was applied, enough to reach saturation in the films. Spin-flip scattering, indicative of magnetization perpendicular to the applied field, was thus not observed. As typical examples, the top panels of Fig. 3 show the non-spin-flip reflectivities (R^{++} for spin up and R^{--} for spin down) for $t_A = 2.7$ nm at 300 K and for $t_A = 4.3$ nm at 6 K (for the sake of clarity R^{--} was multiplied

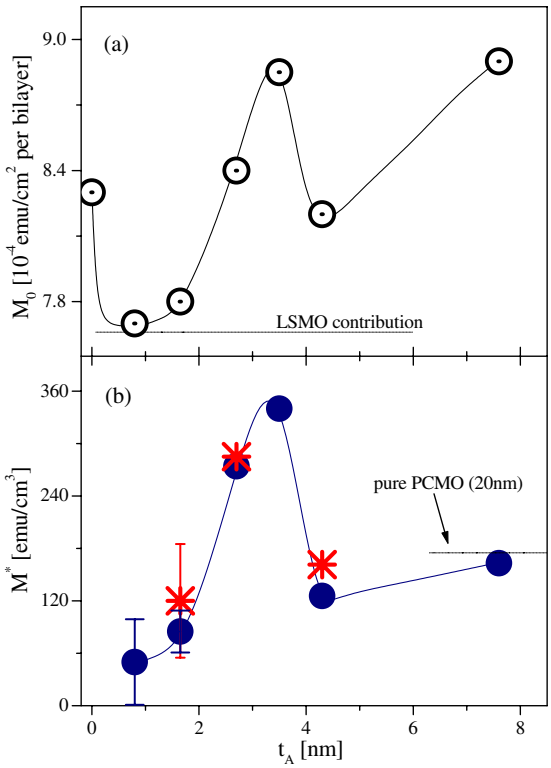

FIG. 2 (color online). (a) Total FM moment of the samples at 5 K as a function of t_A. The horizontal line is the contribution of the LSMO layers for $t_A > 0$. (b) FM moment of the $Pr_{2/3}Ca_{1/3}MnO_3$ layers only. The dotted line shows the FM moment of a 20-nm-thick PCMO film. The FM moment obtained from PNR at 6 K is also shown (star symbols). Only error bars bigger than the symbols are shown.

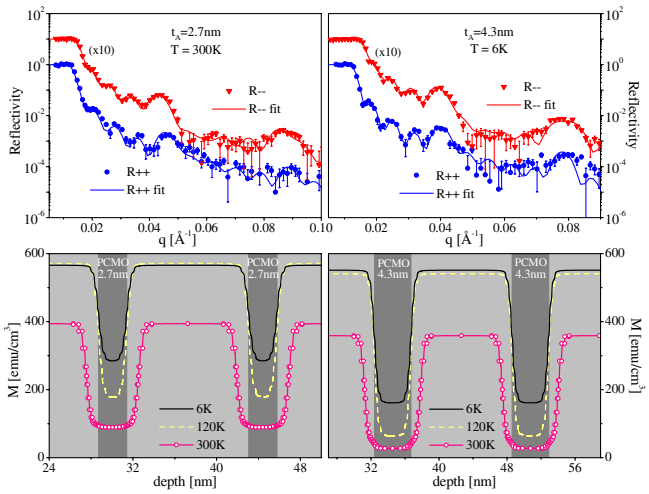

FIG. 3 (color online). Top: Neutron reflectivity for the samples with $t_A = 2.7$ nm (at 300 K, left) and $t_A = 4.3$ nm (at 6 K, right). Triangles and circles correspond to R^{--} and R^{++}, respectively (R^{--} was multiplied by 10). The solid lines through the data are the fits. Bottom: M profiles at the three studied temperatures for the same samples ($t_A = 2.7$ and 4.3 nm on the left and right sides, respectively). The light and dark gray areas are the LSMO and PCMO layers, respectively.

by 10). Note that the q-dependent splitting between the non-spin-flip reflectivities at wave vectors above the total reflection edge ($q \geq 0.014$ Å^{-1}) is sensitive to the depth-dependent projection of the magnetization parallel to the field. Using the REFLPAK software suite [15], the data were fitted to models for the depth profile of the structure and magnetization after correcting for polarization efficiencies ($> 97\%$) and other instrumental effects. The models used to fit these data were kept as simple as possible, while keeping a high quality fit. We note that the quality of the PNR data for $t_A = 1.7$ nm is reduced relative to that obtained for the other two samples studied due to limitations in measurement time and in counting statistics. These data are not shown in the interest of space, but they were fit successfully with parameters that are consistent with the magnetization results as well as with the other two samples (see below).

The obtained M profiles for $t_A = 2.7$ and 4.3 nm are shown in the bottom panels of Fig. 3. For all three samples, the fits at 300 K show the presence of 1.2-nm-thick regions on the LSMO side of the interfaces where M is widely suppressed as compared to the inner volume of the LSMO layers, the so-called magnetically disordered interfaces (MDIs). While MDIs are easily distinguished at 300 K, at low T they are not clearly visible in the PNR model fits. This means that the low-T MDIs must be narrower than 0.5 nm (the roughness of the interfaces and the depth resolution limits of PNR mask the reduced magnetization on this length scale). Actually, previous works on similar manganite systems also show MDIs at the nanometer scale at high T [13,14,16,17], while at low T the disordered regions become unobservable. On the other hand, the drop of M_0 at 5 K between the pure LSMO sample ($t_A = 0$) and $t_A = 0.8$ nm requires the presence of MDIs with a thickness of at least 0.4 nm. Then, with MDIs of $\sim$0.4–0.5 nm the FM contribution of the LSMO to the magnetic moment of the superlattices must be ~ 7.6–7.7×10^{-4} emu/cm^2 per layer [the dashed line in Fig. 2(a) indicates 7.65×10^{-4} emu/cm^2 per layer].

Magnetically disordered regions have been observed at interfaces as well as at the free surface of manganites [16,17]. In $La_{0.7}Sr_{0.3}MnO_3$ films, spin-resolved photoemission spectroscopy (SPES) shows that, while at low T full saturation is reached, at higher T (below T_C) several Mn-O layers at the free surface of the film exhibit a reduced magnetization as compared to the material underneath [16]. This agrees with the observation that the MDIs are regions where M decays faster with T, thus deteriorating the TMR [1]. Also in our PNR experiments the MDIs are more clearly observed at higher T (Fig. 3), but even at low T these disordered interface regions introduce anomalous features in our $M(H)$ data. As shown in the inset of Fig. 1 for $t_A = 0$ and 0.8 nm, the magnetization reversal when H changes sign consists of two steps: first, a fast reversal occurs at $\mu_0 H < 5$ mT, followed by a more gradual moment increase at higher fields. For both samples the fast reversal is similar, with the same values of M. However, at higher fields the magnetization for $t_A = 0.8$ nm stays clearly lower than for $t_A = 0$, indicating that full saturation is not reached. Since the difference between the two samples is the contact of the LSMO surfaces with PCMO, this behavior must be related to the interfaces. We conclude that the sharp reversal corresponds to the inner volume of LSMO in the films, while the gradual increase of M is related to the alignment of the disordered LSMO surfaces. At low T, full saturation can be reached in the free LSMO surfaces in high fields, as observed in SPES experiments [16]. However, when the LSMO surfaces are in contact with PCMO the MDIs remain disordered in fields as large as 7 T and the magnetic moment is smaller. We thus speculate that the PCMO moments at the interfaces pin the magnetic moments of the already disordered LSMO surfaces.

After its initial decrease, M_0 increases again for PCMO thicknesses above 0.8 nm and a second feature develops, i.e., a maximum at intermediate t_A. It is well known that PCMO is phase separated on the nanoscale, either in bulk or thin films [7–9]. Indeed, we prepared a 20-nm-thick PCMO film which exhibits spontaneous ferromagnetism. Its FM moment $\sim$175 emu/cm^3 is superposed to the linear M-H response of the predominant AFM background. In the multilayers, the FM moment of the PCMO layers (M^*) was obtained as a function of t_A after subtracting the contribution from the LSMO [see Fig. 2(b)].

The maximum of M_0 now appears as a maximum in M^* vs t_A. For very small t_A (< 2 nm) the FM moment of PCMO remains small, below 80 emu/cm^3. Presumably, the thin PCMO layers are not large enough to accommodate FM clusters, and only a small number of them can form. For large t_A, M^* approaches the magnetization of the pure PCMO film (thickness 20 nm). In between, the pronounced peak of M^* at t_A around 3 nm is confirmed by the PNR experiments. When we compare the magnetic profiles of the samples at 6 K, the magnetization in the LSMO layers is observed to be nearly the same, and corresponds to the saturation of LSMO (solid lines in the bottom panels of Fig. 3). The T dependence of M in the LSMO layers is also similar for all the samples (square symbols in Fig. 4). However, the FM moment inside the PCMO layers is clearly largest in the 2.7 nm sample. Moreover, as demonstrated in Figs. 2(b) and 4, the values obtained from PNR at 6 K are in very good agreement with those calculated from $M(H)$ at 5 K. This maximum FM contribution of the PCMO layers may originate from an increased population of FM clusters within the AFM matrix at intermediate thicknesses. Of course, PNR does not provide information about the size or characteristics of these clusters since the depth-dependent M profile is an average of the FM moment across the film plane.

The cause of the increase of the PCMO FM moment is not obvious. On one hand, the proximity of the LSMO FM

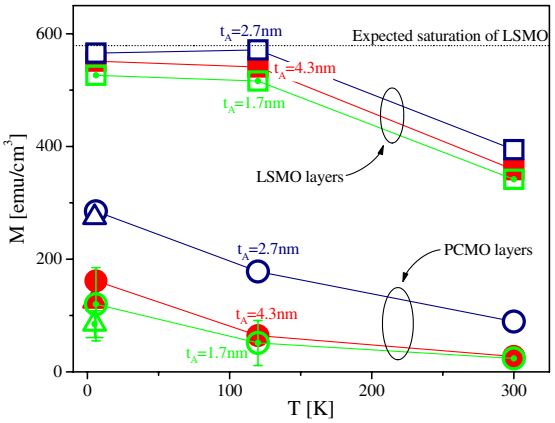

FIG. 4 (color online). Temperature dependence of the FM moment of the different layers of the LSMO/PCMO superlattices, as obtained from PNR. The triangles are the magnetic moments of the PCMO layers deduced from the magnetization measurements at $T = 5$ K [M^*, see Fig. 2(b)]. Only error bars bigger than the symbols are shown.

layers may induce FM correlations inside the PCMO [4,18]. However, any interface magnetic coupling should be precluded by the MDIs. But even at 300 K with 1.2-nm-thick MDIs, the maximized FM moment of PCMO for $t_A = 2.7$ nm persists (see Figs. 3 and 4). On the other hand, the modified physical properties of thin manganite films point to the relevance of interface clamping and lattice strain in these samples [2,3,5,19]. Moreover, strain effects have been linked with nanoscopic as well as mesoscopic phase separation in many manganite samples [8,20], including thin films. Indeed, a FM contribution of the PCMO layers at 300 K is highly unusual. At this T a FM response is totally absent in bulk PCMO; thus, possibly growth-induced strain fields may play a key role for the stabilization of FM nanoclusters in our films. Finally, cation disorder and charge segregation are also possible sources for nanoscale phase separation [6,8]. Unfortunately, the microscopic origin of the t_A dependence of M^* cannot be uniquely determined from our current experiments. Our results, however, show clearly that the optimization of the FM moment of PCMO is driven by the geometrical confinement of the FM clusters within thicknesses $t_A \sim 3$ nm. Since neutron scattering experiments show a similar length scale for the size of the FM clusters [9], the accommodation of these clusters within the PCMO is likely to be favored by the matching condition between layer thickness and FM cluster size.

In summary, the combination of PNR and magnetometry reveals the nanoscale magnetic structure of the LSMO/PCMO multilayers. The stacking of PCMO on top of LSMO hampers the saturation at the surfaces of the ferromagnetic LSMO layers, forming 1.2-nm-thick magnetically disordered interfaces at 300 K. In the phase-separated PCMO, a maximum FM moment occurs for layer thicknesses comparable to the characteristic correlation length of the FM nanoclusters, i.e., for $t_A \sim 3$ nm. This enhancement of ferromagnetism in the nominally AFM spacer could have important implications for the TMR response of these devices. In similar manganite multilayers the TMR can be optimized at intermediate thicknesses [2,3]. In our superlattices, our ability to maximize the FM moment implies that optimization and manipulation of the electronic properties of the insulating spacer may be achieved by controlling its layer thickness.

*Present address: School of Natural Sciences and Mathematics, The University of Texas at Dallas, Richardson, TX 75083-0688, USA.

[1] M. Ziese, Rep. Prog. Phys. **65**, 143 (2002); M. Viret *et al.*, Europhys. Lett. **39**, 545 (1997); M. Jo *et al.*, Appl. Phys. Lett. **75**, 3689 (1999); V. Garcia *et al.*, Phys. Rev. B **69**, 052403 (2004); M. Jo *et al.*, *ibid.* **61**, R14 905 (2000); Y. Lu *et al.*, *ibid.* **54**, R8357 (1996).
[2] R. Cheng *et al.*, Appl. Phys. Lett. **72**, 2475 (1998).
[3] H. Li *et al.*, Appl. Phys. Lett. **80**, 628 (2002); A. Venimadhav *et al.*, J. Phys. D **33**, 2921 (2000).
[4] I. N. Krivorotov *et al.*, Phys. Rev. Lett. **86**, 5779 (2001).
[5] M. Jo *et al.*, J. Phys. Condens. Matter **15**, 5243 (2003).
[6] E. Dagotto *et al.*, Phys. Rep. **344**, 1 (2001); Y. Tokura and Y. Tomioka, J. Magn. Magn. Mater. **200**, 1 (1999).
[7] V. N. Smolyaninova *et al.*, Phys. Rev. B **65**, 104419 (2002); M. S. Reis *et al.*, *ibid.* **71**, 144413 (2005).
[8] P. G. Radaelli *et al.*, Phys. Rev. B **63**, 172419 (2001).
[9] D. Saurel *et al.*, Phys. Rev. B **73**, 094438 (2006); S. Mercone *et al.*, *ibid.* **68**, 094422 (2003).
[10] A tiny magnetic contribution was found in the clean STO substrates. This could be due to 1–2 ppm of Fe impurities that are present even in the best STO crystals available.
[11] D. Niebieskikwiat *et al.*, J. Magn. Magn. Mater. **237**, 241 (2001); Phys. Rev. B **63**, 212402 (2001).
[12] S. S. P. Parkin *et al.*, Phys. Rev. Lett. **64**, 2304 (1990); C. F. Majkrzak *et al.*, *ibid.* **56**, 2700 (1986).
[13] A. Hoffmann *et al.*, Phys. Rev. B **72**, 140407(R) (2005); S. Park *et al.*, *ibid.* **70**, 104406 (2004); J. A. C. Bland *et al.*, *ibid.* **57**, 10272 (1998).
[14] J. Chakhalian *et al.*, Nature Phys. **2**, 244 (2006).
[15] P. A. Kienzle *et al.*, http://www.ncnr.nist.gov/reflpak.
[16] J.-H. Park *et al.*, Phys. Rev. Lett. **81**, 1953 (1998).
[17] J. W. Freeland *et al.*, Nat. Mater. **4**, 62 (2005).
[18] I. Panagiotopoulos *et al.*, J. Appl. Phys. **85**, 4913 (1999).
[19] M. Izumi *et al.*, Phys. Rev. B **61**, 12187 (2000); Z. Q. Yang *et al.*, Appl. Phys. Lett. **88**, 072507 (2006).
[20] J. Tao *et al.*, Phys. Rev. Lett. **94**, 147206 (2005); M. Bibes *et al.*, *ibid.* **87**, 067210 (2001); K. H. Ahn *et al.*, Nature (London) **428**, 401 (2004).